Behavior of structural macrosynthetic fiber-reinforced precast, prestressed hollow-core slabs at different flexure-to-shear ratios

Pradeep Kankeri, Sameer K. S. Pachalla, Nikesh Thammishetti, and S. Suriya Prakash

- Benefits of adding macrosynthetic fiber to concrete for structural improvements, particularly related to hollow-core slab applications, are reviewed in this paper.
- This includes studying the effects of fiber reinforcement additives for various shear span–to–depth ratios of hollow-core slab specimens.
- The paper reviews available literature related to fiber-reinforced concrete as well as provides results of full-scale testing conducted on hollow-core slabs specimens and reviews the applicability of analytical modeling.

PCI Journal (ISSN 0887-9672) V. 64, No. 3, May–June 2019.
PCI Journal is published bimonthly by the Precast/Prestressed Concrete Institute, 200 W. Adams St., Suite 2100, Chicago, IL 60606.

The main advantages of using precast concrete elements, such as hollow-core slabs, are high quality control and reduced construction time. Hollow-core slabs have longitudinal voids running along the spans, which reduces the slab's weight and creates a more efficient cross section for prestressing. Hollow-core slabs are usually designed as uncracked elements under service loads. However, if a structure is overloaded due to change in use, architectural modifications, or material degradation, these elements can crack and may not meet the required serviceability design criteria. Because hollow-core slabs are produced via an extrusion process, the provision of additional reinforcement is not feasible. In such scenarios, the addition of structural synthetic fibers to the concrete during casting can enhance the performance of the slabs after cracking. Current American Concrete Institute (ACI) codes require at least 60 kg (130 lb) of deformed steel fibers per cubic meter of concrete for shear reinforcement. However, in prestressed hollow-core slabs, the beneficial effect of prestressing forces could relax the minimum fiber volume requirement.

Steel fibers have superior mechanical properties compared with those of synthetic fibers; hence these fibers are commonly used in concrete. However, the steel fibers decrease the workability of the concrete and create balling effects at higher fiber volume dosages in zero-slump concrete, which is generally used for the extrusion of hollow-core slabs. Structural synthetic fibers, being noncorrosive and malleable, have gained attention in recent years and can be used for reinforcing cementitious materials to control crack propagation and improve the overall structural performance. Polyolefin fibers

come under this category of synthetic fibers. They are manufactured in two different types: monofilament and fibrillated. Monofilament fibers are single-strand with the same sectional area throughout their length. Fibrillated fibers are produced as films or tapes that can transform into a net-like physical structure. Monofilament polyolefin fibers are available as microsynthetic and macrosynthetic fibers. Microsynthetic fibers are typically 12 mm (0.5 in.) long and 0.018 mm (0.0007 in.) in diameter, whereas macrosynthetic fibers are significantly larger at 40 to 50 mm (1.6 to 2 in.) in length and 0.3 to 1.5 mm (0.01 to 0.06 in.) in diameter. Macrofibers are generally used to enhace the capacity of the elements, whereas microfibers are used to control shrinkage cracks.

The focus of this investigation is to study the effects of structural macrosynthetic fiber reinforcement on the cracking and ductility behavior of prestressed hollow-core slabs at different levels of shear span–to–depth ratio *a*/*d* (where *a* is the shear span and *d* is the depth of the section) or flexure-to-shear levels. This study includes a literature review as well as full-scale testing and analytical predictions.

Literature review

Steel-fiber-reinforced concrete

In the past few decades, researchers have used fibers as secondary reinforcement in concrete elements. Cuenca et al.[1] used steel fibers to control crack propagation in precast concrete beams. The authors found that the fibers and stirrups had a synergistic effect in increasing the strength of beams. Cuenca and Serna[2] have investigated the influence of the concrete matrix and type of fiber on the shear behavior of self-consolidating fiber-reinforced concrete beams. The authors considered two different concrete compressive strength values and five different types of steel fibers to evaluate the shear behavior of reinforced concrete beams. The authors found that the type of fibers used substantially affected the shear behavior. The authors also found that a combination of high-strength concrete with low-strength fibers was not very efficient in improving performance. Martinola et al.[3] used fibers for external strengthening in the form of concrete jackets for reinforced concrete beams and found that the fibers are very effective for the repair and external strengthening of reinforced concrete beams. The flexural capacity and shear capacity of prestressed concrete beams with steel fibers were predicted by various authors (Padmarajaih and Ramaswamy[4] and Narayanan and Darwish[5]) by developing analytical models suitable for various volumes of fibers. Although numerous researchers have focused on fiber-reinforced concrete (FRC) in the past, the effect of synthetic fiber reinforcement on the flexure and shear behavior of hollow-core slabs has not been explored in detail.

Prestressed hollow-core slabs

Various researchers have studied the effects of hollow-core slab depth and shear span–to–depth ratio *a*/*d* on the capacity of hollow-core slabs. They have evaluated the behavior and shear strength of hollow-core slabs and suggested various modifications to the existing code equations for capacity predictions.[6–9] Previous studies[10–13] have found that the performance of prestressed hollow-core slabs improves with the addition of steel fibers to the concrete during casting. Peaston et al.[12] observed that the cracking and peak loads of FRC hollow-core slabs are higher than those of control slabs with no fibers. The authors observed that at relatively low *a*/*d* values, the ACI 318 equations accurately predicted the shear strength of hollow-core slabs without the addition of fibers. However, when modified for steel fiber by other researchers, the ACI equations were found to overestimate the strength of fiber-reinforced hollow-core slabs. Cuenca and Serna[14] conducted an experimental program on hollow-core slabs with different test variables, including amount of steel fibers (0, 50, and 70 kg/m^3 [0, 84, and 118 lb/yd^3]) and *a*/*d* values of 2.3, 4.4, and 8.6. The authors observed that hollow-core slabs with fibers could resist greater loads than the control slabs and with a more ductile behavior. Marazzini and Rosati[15] studied individual beams cut out of hollow-core slabs with and without steel fibers and found that steel-fiber-reinforced beams have a tendon-to-concrete bond about twice that of beams without fibers for high-strength concretes in the range of 80 to 130 MPa (12 to 19 ksi).

The authors also observed that the post-peak behavior of fiber-reinforced specimens improved without sudden load drops compared with the post-peak behavior of concrete without fiber reinforcement. Jain et al.[16] and Srikar et al.[17] evaluated the effect of steel fibers with different dosages on the strength of concrete and confirmed the increase in ductility in the compressive behavior of concrete. Previous studies by the authors of this paper[18–21] highlight the effect of *a*/*d* on the behavior of hollow-core slabs both with and without strengthening. The increase in strength was observed to depend on various factors, such as *a*/*d* and the compressive and tensile strengths of the concrete. Joshi et al.[22] studied the effects of steel and polyolefin fibers on the flexure-shear behavior of prestressed concrete beams and found that the strength of concrete increased by up to 10% due to the addition of 1% macrosynthetic fibers.

Previous studies have confirmed that the addition of steel fibers increases the peak load and ductility of hollow-core slabs at varying levels. The main disadvantages of using steel fibers are reduced workability, corrosion of steel fibers, handling difficulties, and balling effects at high fiber-volume additions. These problems are aggravated for hollow-core slabs because zero-slump concrete is used for the extrusion process.

To overcome the problems associated with steel fibers, structural synthetic fibers were used in this study. The present study examines the effects of structural synthetic fibers on the behavior of hollow-core slabs. No previous investigation has focused on the effects of structural synthetic fibers on the behavior of hollow-core slabs at different *a*/*d* values.

Macrosynthetic fiber-reinforced concrete

Mechanical properties, including the compressive and tensile strength of FRC (both steel and synthetic), have been relatively well studied (Olivito and Zuccarello,[23] Soulioti et al.,[24] Barros and Fueiras,[25] and Li[26]). Rasheed et al.[27] found that the addition of polypropylene fibers marginally increased flexural tensile strength. The fibers were found to greatly increase the ultimate strain, but there was a decrease in load-carrying capacity. In their experiments on polypropylene fiber-reinforced beams, Cifuentes et al.[28] found that the effect of the fiber was more significant for low-strength concrete, which was attributed to the stresses in a cohesive zone that is directly proportional to the strength of concrete. The investigation by Lanzoni et al.[29] suggested that even a low dosage of synthetic fibers effectively reduces crack formation and growth to an extent comparable to that of steel fibers.

Research significance and objectives

Hollow-core slabs are usually designed to be uncracked under full service load.[30] A major issue in the serviceability performance of the hollow-core section is that flexural cracks propagate more rapidly through the thin curved webs than they otherwise would in a rectangular section. Also, tension stiffening of concrete is not as effective due to the absence of regular reinforcement other than prestressing strands and the transition from a flexurally uncracked section to a flexurally cracked section is rapid in hollow-core slabs; thus the shape of the cross section accelerates crack propagation and reduces postcracking stiffness and ductility. The available literature indicates that the addition of both steel and synthetic fibers improves the strength and behavior of reinforced and prestressed concrete members significantly. Many studies have shown this effect quantitatively. No previous work has evaluated the behavior of prestressed hollow-core slabs with structural synthetic fibers as secondary reinforcement and its effect on the strength, ductility, cracking, and failure mode of these slabs. Understanding this behavior is particularly important because of the zero-slump mixture proportion used for extrusion of the slabs and the absence of any reinforcement other than prestressing strands. Moreover, the influence of synthetic fibers on the flexure, shear, and flexure shear behavior of prestressed hollow-core slabs at different *a*/*d* values is also not clear. Kani[31] investigated the effect of different *a*/*d* values on the fundamental behavior of reinforced concrete beams. The author found that the reinforced concrete beams had dominant flexure behavior above an *a*/*d* of 6. The author also observed that there is a transition region between the *a*/*d* values of 2.5 and 3.0, below which the beams are shear critical and the corresponding bending moment at failure was found to be low. Below an *a*/*d* of 2.5, the beam developed an arch action with a considerable reserve strength beyond the first cracking point. Similarly, for an *a*/*d* between 2.5 and 5, the failure was due to diagonal shear tension. However, these results are from tests on reinforced concrete beams, and their applicability to hollow-core slabs with different cross-section details may not be strictly valid. This paper examines the behavior of synthetic fiber-reinforced hollow-core slabs with respect to strength, failure modes, and serviceability performance at various flexure-to-shear levels or *a*/*d* values. For consideration in future work, investigations may include the effects of fiber volume fraction, different support conditions, cross-section details, and size effect on the behavior of fiber-reinforced prestressed concrete beams.

Experimental investigation

Six hollow-core slabs were tested to evaluate the effects of macrosynthetic fibers on load-displacement behavior. **Table 1** presents the details of the test specimens. Specimens are denoted using the following nomenclature: for HCS-150-3.75-3, HCS denotes hollow-core slabs, 150 denotes the depth of the slab in millimeters, 3.75 denotes the *a*/*d*, and 3 represents the dosage of fiber. The primary variable considered was *a*/*d*. The slabs were 3100 mm (122 in.) in length and 150 mm (6 in.) in thickness. The slabs were tested at three different *a*/*d* values—2.5, 3.75, and 7.5—to show the effects of fiber addition on the behavior of slabs under different dominant conditions. Two slabs, one without fibers and one with fibers, were tested at each *a*/*d* value. The test slabs without fibers were considered to be the control specimen for each *a*/*d* value. All slabs had the same geometry (**Fig. 1**). The tested slabs were cut to a 600 mm (24 in.) width from a full-sized 1200 mm (48 in.) wide hol-

Table 1. Details of hollow-core slab test specimens

Specimen number	Specimen label	Specimen depth *d*, mm	Shear span–to–depth ratio *a*/*d*	Fiber content, kg/m³	Volume fraction, %
1	HCS-150-2.50-0	150	2.50	0	0
2	HCS-150-2.50-3	150	2.50	3	0.33
3	HCS-150-3.75-0	150	3.75	0	0
4	HCS-150-3.75-3	150	3.75	3	0.33
5	HCS-150-7.50-0	150	7.50	0	0
6	HCS-150-7.50-3	150	7.50	3	0.33

Note: HCS = hollow-core slab. 1 mm = 0.0394 in.; 1 kg/m³ = 1.6855 lb/yd³.

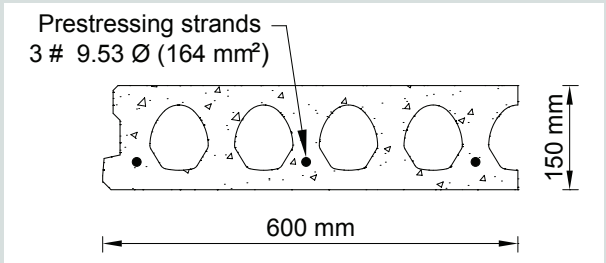

Figure 1. Cross-section details of hollow-core slab. Note: 1 mm = 0.0394 in.; 1 mm² = 0.00155 in.²

low-core slab. The slabs were prestressed with three 9.53 mm (0.375 in.) diameter strands with a prestressing force of 70 kN (15.7 kip) each. The prestressing force in the strands induced a compressive stress of 7.3 MPa (1.1 ksi) at the bottom layer of the section, which is 17.3% of the characteristic compressive strength of concrete used. Polyolefin macrosynthetic fibers were added to three of the test slabs during casting. The dosage of fibers added was 3 kg/m³ (5 lb/yd³) of concrete corresponding to a fiber volume fraction of 0.33%, which was chosen based on the previous research and published test results.[14,27] From the previous results, it was observed that the addition of fibers from 3 to 6 kg/m³ (5 to 10 lb/yd³) would have a similar increase in peak load. Although a higher dosage of fibers can yield better post-peak behavior, a lower fiber dosage of 3 kg/m³ was chosen based on the workability of zero-slump concrete used for extrusion of these slabs. All slabs were cast on the same day and were cured for the same duration. Table 1 shows the overall test matrix with the study parameters.

Material properties

Concrete All specimens were cast using normalweight concrete designed to have a target design compressive strength of 40 MPa (5.8 ksi) at 28 days. Coarse aggregates of 10 mm (0.4 in.) nominal size along with fine aggregates were used in the mixture to enable casting through an extrusion process. The unit weight of concrete was 2400 kg/m³ (4050 lb/yd³). The tested average concrete strength was 43 MPa (6.2 ksi) at 28 days with a standard deviation of 0.8 MPa (0.1 ksi).

Table 2. Properties of polyolefin fibers

Material	Polyolefin
Form	Structural macrosynthetic monofilament fiber
Specific gravity	0.91
Length, mm	50
Diameter, mm	0.5
Tensile strength, MPa	618
Modulus of elasticity, GPa	10

Note: 1 mm = 0.0394 in.; 1 MPa = 0.145 ksi; 1 GPa = 145 ksi.

Structural polyolefin macrosynthetic fibers Structural polyolefin fibers that were 50 mm (2 in.) in length and 0.50 mm (0.02 in.) in diameter were added to the concrete during casting (**Table 2**). The fibers had a modulus of elasticity of about 10 GPa (1450 ksi) and tensile strength between 550 and 640 MPa (80 and 93 ksi). The fibers had a continually embossed surface anchorage mechanism to enhance bond. Uniform distribution of fibers was observed during casting. Cracked surfaces of the specimens were examined after failure, and an even distribution of fibers was observed.

Behavior of synthetic fiber-reinforced concrete under compression As part of an extended study,[22] cylinders

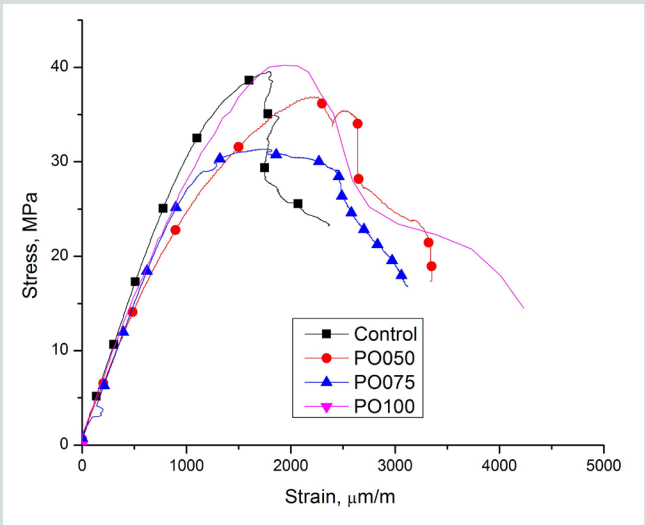

Stress-strain curves of concrete under compression

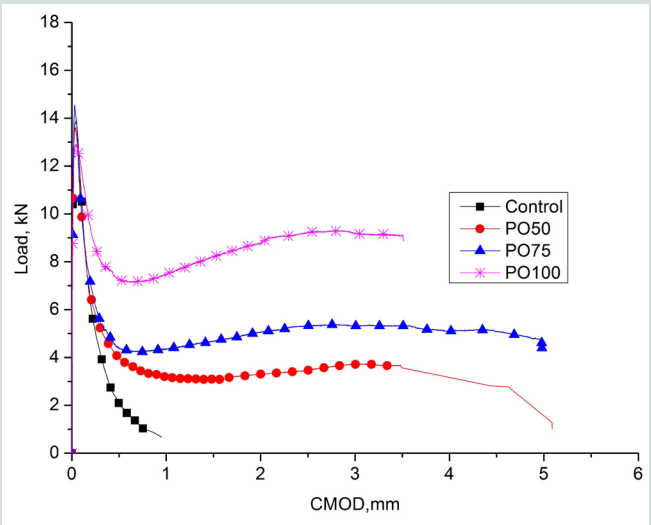

Load-CMOD behavior of polyolefin fiber-reinforced concrete

Figure 2. Material characterization of macrosynthetic fiber-reinforced concrete. Note: CMOD = crack mouth opening displacement. 1 mm = 0.0394 in.; 1 m = 3.281 ft; 1 kN = 0.225 kip; 1 MPa = 0.145 ksi.

cast with concrete of different fiber dosages were tested to understand the effect of fibers on the stress-strain behavior of concrete under compression. The addition of fibers was found to improve the compressive strength and stiffness degradation in the post-peak region with better ductility (**Fig. 2**). The author's previous work, which contains further details of this study, has also confirmed the same at both the room and moderate temperature exposure.[16,17,22]

Fracture behavior of synthetic fiber-reinforced concrete Previously, limited research has focused on the fracture behavior of synthetic fiber-reinforced concrete, limiting its widespread use in infrastructure applications. The residual load-bearing capacity is measured by fracture tests. The efficiency of structural fiber can be measured based on the fracture behavior. Synthetic fibers offer considerable residual tensile strengths, and their contribution can be considered in the structural design. A three-point bending test was performed on simply supported notched beams to understand the effect of fibers on the fracture behavior of concrete.[22] Three different fiber dosages by volumes were considered: 5 kg/m^3 (8.4 lb/yd^3) labeled PO50, 7.5 kg/m^3 (12.7 lb/yd^3) labeled PO75, and 10 kg/m^3 (16.8 lb/yd^3) labeled PO100. Figure 2 shows the fracture behavior. The effect of polyolefin macrosynthetic fibers can be quantified either in terms of areas under the load-deflection curve or by the load-bearing capacity at a certain deflection or crack mouth opening displacement (CMOD). Figure 2 presents the load-CMOD behavior of the beams. It shows that the area under the curve increases with the increase in the fiber dosage. The test results show that synthetic fibers improved the residual strength for small deformations and that they can enhance the structural performance of hollow-core slabs.

Internal reinforcement: Prestressing steel strands Seven-wire low-relaxation strands with a 9.53 mm (0.375 in.) diameter, ultimate tensile strength of 1860 MPa (270 ksi), and modulus of elasticity of 196.5 GPa (28,500 ksi) were used as prestressing strands. Strands were placed at an effective depth of 125 mm (5 in.), and a prestressing jacking force of 70 kN (15.7 kip) was applied to each of the strands.

Instrumentation

Instrumentation was done to measure the effects of the addition of fibers to the hollow-core slab specimens. Strain gauges were instrumented on the prestressing strands to measure strain variations during the test. All specimens had similar instrumentation details. Deflections were recorded using linear variable displacement transducers (LVDTs). Specific LVDT locations were chosen to capture the entire curvature profile during testing. Two 50 mm (2 in.) LVDTs were positioned at one-third of the clear span distance, and one 100 mm (4 in.) LVDT was positioned at the center of the span to capture midspan deflection. Strain gauges with a gauge length of 120 mm (4.7 in.) were used to measure the strains in the concrete. The surface was thoroughly cleaned, and the strain gauges were installed on the top and bottom of the concrete slab to capture the strain profile across the section. Strain gauges with a 5 mm (0.02 in.) gauge length were instrumented on the prestressing strands to capture the strain variation in the strands during testing. A data acquisition system was used to capture the data from the external instrumentation.

Test setup and loading details

The slabs were tested in a four-point bending configuration. **Figure 3** illustrates the components used in the test setup. A 250 kN (56.2 kip) hydraulic actuator was used to apply loads. The actuator load was transferred to the concrete slab specimens via a single longitudinal rigid steel spreader beam stiffened with web stiffeners. The load from the spreader beam was transferred to the slab through two transverse I-beams as two distributed line loads along the full width of the slab. High-strength cement mortar was used between the two transverse spreader I-beams and the slab to eliminate surface irregularities and to avoid stress concentrations. The end supports included I-beams with transverse stiffeners to avoid any local buckling. Loading was applied monotonically in displacement control mode at a rate of 0.05 mm/sec (0.002 in./sec). Loading was paused intermittently to observe and mark the cracks, which were used to understand the failure progression.

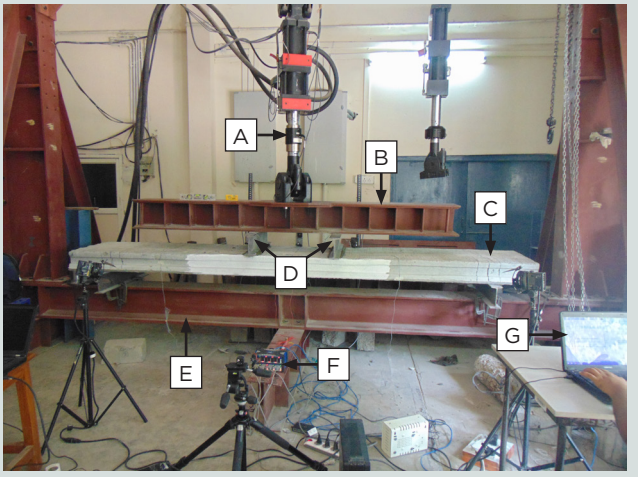

Figure 3. Test setup. Note: A = 250 kN (56 kip) actuator; B = spreader beam; C = hollow-core slab; D = transverse I-beams; E = support I-beams; F = data acquisition system; G = laptop.

Test results and discussion

Load-deflection behavior

The shear capacity of hollow-core slabs is considered to be satisfactory for most building applications. However, the lack of ductility in the post-peak regime is a major concern; thus the effects of adding synthetic fibers on the shear resistance and ductility of the hollow-core slabs were investigated at different *a*/*d* values. **Figure 4** shows the deflection response versus load of the tested slabs. The elastic response of the slabs with the same *a*/*d* was found to be similar because the

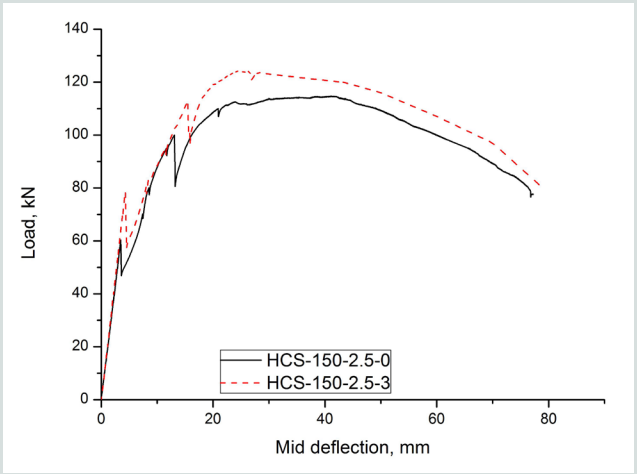

a/d = 2.50

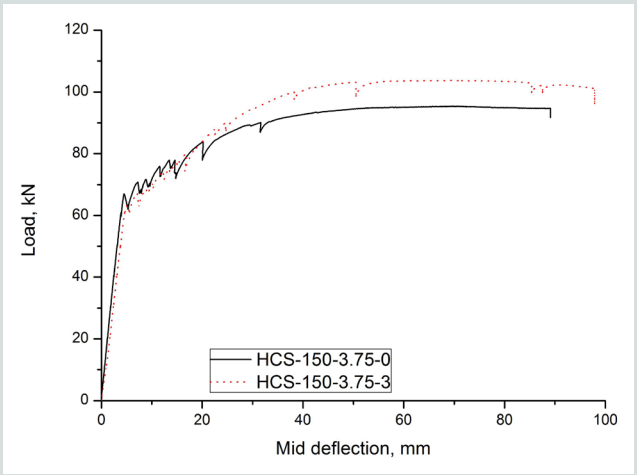

a/d = 3.75

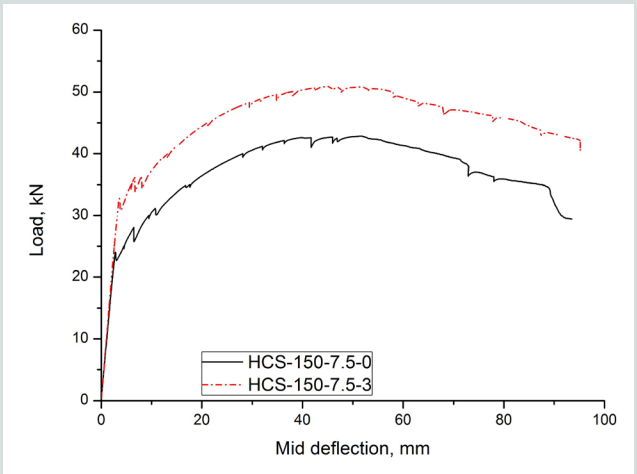

a/d = 7.50

Figure 4. Load versus deflection behavior of hollow-core slab specimens at shear span–to–depth ratios *a/d* of 2.5, 3.75, and 7.5. Note: 1 mm = 0.0394 in.; 1 kN = 0.225 kip.

initial response depends entirely on the flexural rigidity of the slab. After the crack initiation, there was a change in the slope of the load-deflection curve and all tested slabs had different ductility before reaching failure. The specimen HCS-150-2.50-0 was tested at an *a/d* of 2.5. Initial cracking occurred at a load of 60.3 kN (13.6 kip) at a deflection of 3.5 mm (0.14 in.). After cracking, there was a sudden drop in load from 60.3 to 47 kN (13.6 to 10.6 kip). On further loading, there was intermittent cracking and the slab reached a peak load of 115 kN (25.85 kip) at a deflection of 41 mm (1.6 in.). The slab finally failed due to diagonal shear tension.

Specimen HCS-150-2.50-3, which had fibers at a dosage of 3 kg/m^3 (5 lb/yd^3) and was tested at an *a/d* of 2.5, exhibited behavior similar to that of the control slab in the elastic region. The cracking load of the fiber-reinforced specimen increased to 78.5 kN (17.6 kip), and the peak load increased to 124.5 kN (28 kip). The addition of fibers increased the ultimate capacity by about 8.3%. This fiber-reinforced slab also failed in diagonal shear tension mode, but it exhibited better postcracking behavior compared with the control slab (**Table 3**). Higher fiber dosage could have helped to convert the failure mode to flexure for the specimen with *a/d* of 2.5; this is an area for further investigation.

A second control slab (HCS-150-3.75-0), with an *a/d* of 3.75, had initial flexural cracking at a load of 67 kN (15 kip) at a corresponding deflection of 4.5 mm (0.17 in.). The load-deflection curve in Fig. 4 and the strain data in Table 3 showed that slab HCS-150-3.75-0 had considerable yielding of strands before reaching the peak load of 95.5 kN (21.5 kip). The slab finally failed due to the crushing of concrete under the loading point. The addition of fibers to the slab tested at an *a/d* of 3.75 (HCS-150-3.75-3) increased the peak load to 104 kN (23.4 kip), a 9% increase compared with the control slab for an *a/d* of 3.75 without any change in its corresponding displacement.

Slabs tested at a higher *a/d* of 7.5 to simulate the high flexure-to-shear ratio with and without fibers had a similar initial response. However, due to the addition of fibers, the cracking load was observed to increase by 36%. The increase in peak load was about 18%. Table 3 presents the test results for all the specimens.

One of the important improvements in the response of the slabs, apart from an increase in peak loads, is the increase in postcracking stiffness. Postcracking stiffness is calculated as the ratio of the difference between the peak and cracking loads to their corresponding difference in deflections. This provides a quantitative measurement of the effectiveness of the fibers in bridging the cracks and their contribution in improving the postcracking stiffness. The postcracking stiffness of the hollow-core slabs increased by 42%, 47%, and 10% for slabs tested at *a/d* values of 2.50, 3.75, and 7.50, respectively, due to the addition of structural macrosynthetic fibers. Thus, fibers can significantly improve the serviceability performance of hollow-core slabs in the event of cracking.

Table 3. Test results of hollow-core slabs

Specimen number	1	2	3	4	5	6
Specimen label	HCS-150-2.50-0	HCS-150-2.50-3	HCS-150-3.75-0	HCS-150-3.75-3	HCS-150-7.50-0	HCS-150-7.50-3
Cracking load P_{cr}, kN	60.3	78.5	67	63.2	24	32.8
Deflection at cracking load Δ_{cr}, mm	3.5	4.3	4.5	5	2.8	3.6
Peak load P_{pl}, kN	115.0	124.5	95.5	104	43	51
Increase in P_{pl}, %	n/a	8.2	n/a	8.9	n/a	18.6
Deflection at peak load Δ_{pl}, mm	41	26.5	69.7	68.3	51.3	45.6
Postcracking stiffness $(P_{pl} - P_{cr})/(\Delta_{pl} - \Delta_{cr})$, kN/mm	1.4	2.1	0.43	0.64	0.39	0.433
Increase in postcracking stiffness, %	n/a	42	n/a	47	n/a	10
Strain in prestressing strand at mid-span before cracking, µm/m	5598	5751	5732	5813	5674	5772
Strain in prestressing strand at mid-span at peak load, µm/m	5740	6323	11,970	10,170	14,280	13,650
Strain in prestressing strand in fiber specimen at peak load of control, µm/m	n/a	5610	n/a	8131	n/a	8388

Note: HCS = hollow-core slab; n/a = not applicable. 1 mm = 0.0394 in.; 1 m = 3.281 ft; 1 kN = 0.225 kip; 1 kN/m = 68.5 lb/ft.

Crack distribution and failure modes

Figure 5 shows the crack distribution and failure modes of the tested specimens. For specimens tested at an *a*/*d* of 2.5, the first cracks were observed below the loading point. On further loading, the cracks converted into diagonal shear cracks. Finally, the slabs failed due to diagonal shear tension failure of concrete. Although the specimens failed in shear, considerable ductility was observed due to the low amount of prestressing steel used in this study. For slabs tested at flexure-dominated *a*/*d* values of 3.75 and 7.50, the addition of fibers increased the number of cracks with better distribution in the constant moment region. Moreover, the observed crack widths were smaller at the same load levels with an even distribution in the fiber-reinforced slabs. The final compression failure of concrete in flexure-dominated behavior (*a*/*d* = 3.75 and 7.50) was delayed due to the presence of fibers.

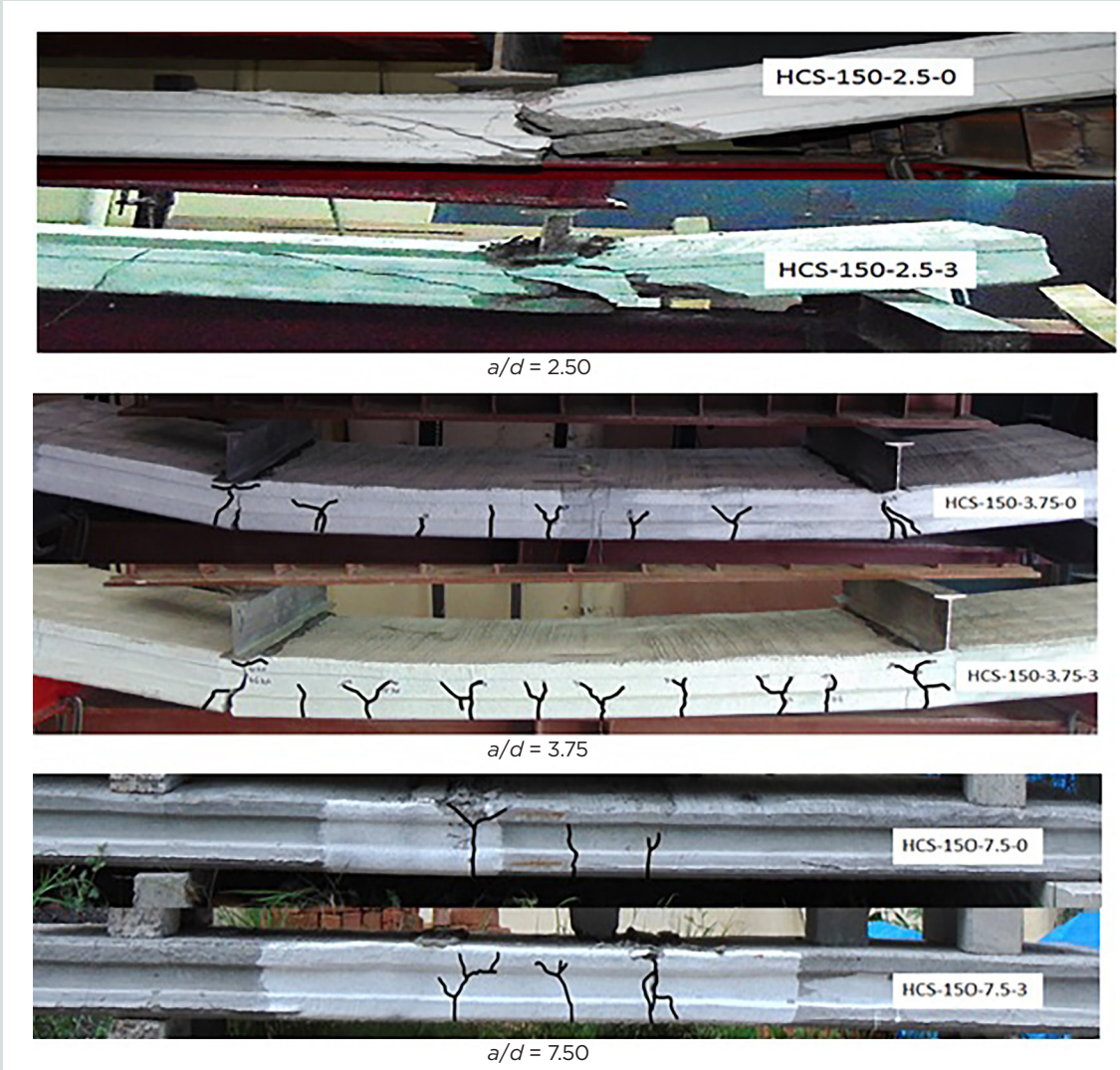

Figure 5. Crack distribution in hollow-core slabs tested at shear span–to-depth ratios *a/d* of 2.5, 3.75, and 7.5.

Load-strain behavior

Strain gauges were mounted on the strands at the midspans of the specimens to measure strain variation during testing. **Figure 6** shows the strain versus load in strands for specimens with an *a/d* of 3.75 and 7.5. Table 3 presents strain values at different load levels for all specimens. The initial strain of 5500 µm/m due to the prestressing force after accounting for losses was supplemented to the measured strain values. Because prestressing strands do not have a well-defined yielding point, a value of 10,000 µm/m was taken as the yielding strain.[32] Figure 6 shows that the strain in the strands increased linearly before cracking. After cracking, an expeditious increase in strain was observed with the increase in load. In the slabs reinforced with fibers, at the same load levels the strain in the strands was found to be less than the strain observed in the control specimens with no fiber reinforcement. The reduction of strain in the strands shows the significant contribution of structural fibers to the load resistance.

The strain versus load plot quantitatively shows the effect of fibers in all tested specimens. Slabs tested at an *a/d* of 2.5 had a shear-dominant failure, and the contribution of the fibers in resisting the shear was marginal. Because no flexural cracks formed in the constant moment zone in the specimens tested at an *a/d* of 2.5, no appreciable increase in strain values was observed; hence the corresponding plot is not presented. **Figure 7** shows the action of fibers in resisting the crack opening and thereby limiting the strains. Table 3 shows that the strain values in fiber-reinforced slabs at peak load is less than the corresponding control slab strains due to the beneficial effect of the fibers.

Strain energy absorption

The strain energy absorption or the energy dissipated can be directly linked to the area under the load-deflection curves, so in this study, the strain energy absorbed by the tested specimens was studied by calculating the area under load-deflection curves. **Table 4** shows the energy dissipa-

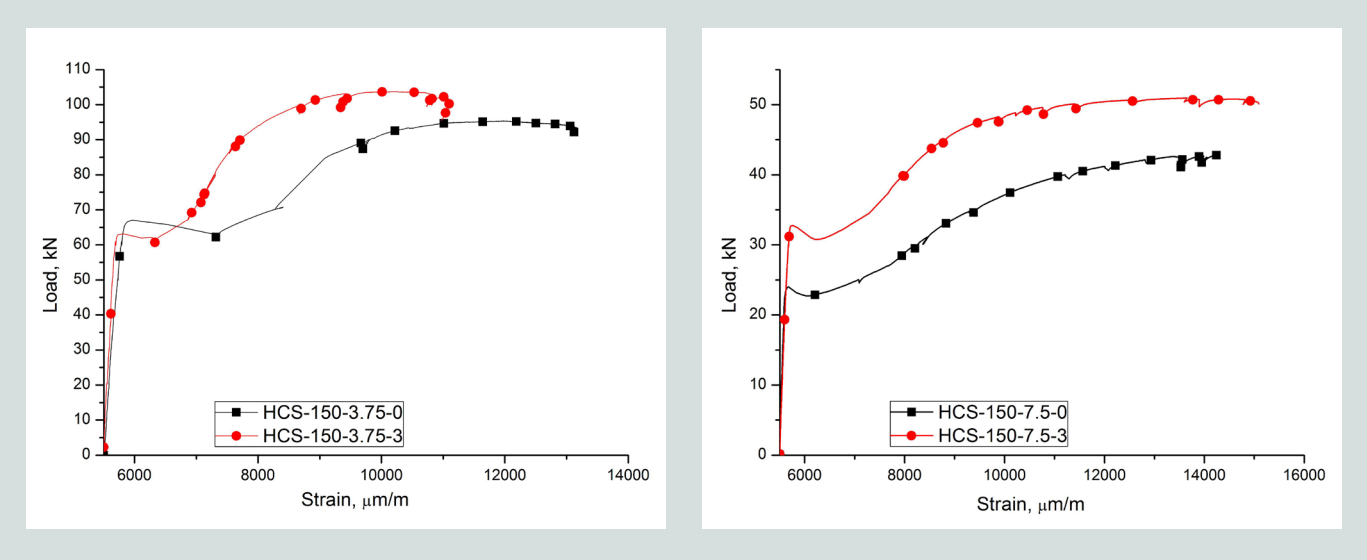

Figure 6. Strain in prestressing strand at midspan. Note: 1 mm = 0.0394 in.; 1 m = 3.281 ft; 1 kN = 0.225 kip.

tion and the percentage increase by the addition of fibers. The addition of fibers increased the energy dissipation in all specimens. A maximum increase of 24% was observed in the slabs tested at an *a*/*d* of 7.5. This increase in strain energy absorption was about 17% and 10% for the slabs tested at *a*/*d* values of 3.75 and 2.5, respectively. The effect of fibers on energy dissipation depends on the *a*/*d* at which the slabs were tested. Strain energy absorption was highest for the slabs with a larger *a*/*d* and gradually decreased with a decrease in *a*/*d*. From the test results presented here, it can be concluded that synthetic fibers enhance flexural resistance more effectively than shear resistance. This can be attributed to the better resistance of the fibers in bridging flexural cracks and reducing the opening of crack widths. Because there were no flexural cracks in the slabs with an *a*/*d* of 2.5, the fibers could not efficiently contribute to crack bridging, leading to less energy absorption at failure. In the slab with an *a*/*d* of 7.5, crack bridging was better because of the flexural cracks, resulting in higher energy dissipation. Because of the lower stiffness of structural macrosynthetic fibers, they may not be as efficient as steel fibers in bridging shear cracks, which are typically wider and propagate faster than flexural cracks.

Fiber distribution

Fiber distribution is the key factor that influences the behavior of fiber-reinforced concrete members. The average fiber spacing is a function of fiber cross-section area, fiber volume, and fiber orientation. When fibers were used in the zero-slump concrete, it affected the flow characteristics of the concrete, which in turn affected the extrusion machine. Taking these constraints into account, the fiber content was restricted to 3 kg/m^3 (5 lb/yd^3). **Figure 8** shows the cross section of the slab after failure. The fibers on the cracked face showed a good distribution across the entire cross section, with no balling effect. Investigating the effect of different fiber dosages is an area for further work.

Table 4. Energy dissipation in tested specimens

Specimen number	Specimen label	Strain energy, kN-mm	Increase, %
1	HCS-150-2.50-0	7493	n/a
2	HCS-150-2.50-3	8281	10.5
3	HCS-150-3.75-0	7731	n/a
4	HCS-150-3.75-3	9073	17.3
5	HCS-150-7.50-0	3444	n/a
6	HCS-150-7.50-3	4272	24.0

Note: HCS = hollow-core slab; n/a = not applicable. 1 kN-mm = 737 lb-ft.

Predictions using analytical models

Although the previous studies[33–37] have developed models to predict the compressive behavior, tensile behavior, and crack width of steel FRC members, models that can predict the behavior of synthetic fibers are still rare. In the present study, the RILEM (International Union of Laboratories and Experts in Construction Materials, Systems and Structures)[38] approach was employed for both the control and synthetic-fiber specimens by modifying the tensile stress-strain curves developed for different reinforcement indices from the load-CMOD plots (Fig. 2). The following section presents the methodology used to obtain the analytical flexural and shear capacities of the hollow-core slabs studied according to RILEM recommendations. **Table 5** compares the analytical and experimental results.

Flexure capacity

An iterative layer-by-layer method of sectional analysis was conducted on an I-section (**Fig. 9**), which is equivalent in terms of cross-section area to the hollow-core slabs tested, to

Tension side (crack arresting of fibers)

Compression side (fibers improve ductility by passive confinement)

Figure 7. Contribution of structural fibers in performance improvement (HCS-150-7.50-3).

predict the flexural capacity of the member. The equivalent I-section is calculated by considering the width of the top flange equal to the overall width of the hollow-core slab and the width of the web is calculated by subtracting the hole diameter from the overall width. In this layer-by-layer sectional analysis, the cross section and corresponding stress-strain curve are discretized into a number of thin layers to obtain the uniform strain throughout the thickness. The analysis begins by considering a value of compressive strain in the top fiber; then the neutral axis depth is iterated to satisfy the force equilibrium. Once the force equilibrium is met, considering the strain distribution, the moment developed in the section is calculated from the moment equilibrium. Table 5 presents the analytical predictions of flexural capacity.

Shear capacity

RILEM[38] gives recommendations for the calculation of design shear resistance of a reinforced concrete or prestressed concrete beam section containing steel fibers and with or without shear reinforcement. Equations (1) through (11) apply to a prestressed fiber-reinforced concrete beam.

$$V_{Rd3} = V_{cd} + V_{fd} + V_{wd} \tag{1}$$

$$V_{cd} = \left[0.12k\left(100\rho_l f_{fck}\right)^{\frac{1}{3}} + 0.15\sigma_{cp}\right]b_w d \tag{2}$$

$$k = 1 + \sqrt{\frac{200}{d}}; k \le 2 \tag{3}$$

$$\rho_l = \frac{A_s}{b_w d} \le 2\% \tag{4}$$

$$\sigma_{cp} = \frac{N_{sd}}{A_c} \tag{5}$$

$$V_{fd} = k_f k_1 \tau_{fd} b_w d(N) \tag{6}$$

Figure 8. Cross section of hollow-core slab showing even macrosynthetic fiber distribution.

$$k_f = 1 + n\left(\frac{h_f}{b_w}\right)\left(\frac{h_f}{d}\right); k_f \le 1.5 \tag{7}$$

$$n = \frac{b_f - b_w}{h_f}; n \le 3 \text{ and } n \le \frac{3b_w}{h_f} \tag{8}$$

$$k_1 = \frac{1600 - d}{1000}; k \ge 1 \tag{9}$$

$$\tau_{fd} = 0.12_{fRk,4} \tag{10}$$

$$V_{wd} = \frac{A_{sw}}{s} 0.9 d f_{ywd}\left(1 + \cot\alpha\right)\sin\alpha \tag{11}$$

where

V_{Rd3} = design shear resistance of a section of a beam

V_{cd} = shear resistance of the member without shear reinforcement

V_{fd} = contribution of the steel fiber shear reinforcement

Table 5. Comparisons of experimental and analytical calculations

Shear span–to-depth ratio *a/d*	2.50		3.75		7.50	
Specimen number	1	2	3	4	5	6
Specimen label	HCS-150-2.50-0	HCS-150-2.50-3	HCS-150-3.75-0	HCS-150-3.75-3	HCS-150-7.50-0	HCS-150-7.50-3
Analytical flexural capacity, kN	147.45	152.29	98.30	101.68	49.15	50.84
Analytical shear capacity, kN	89.79	106.67	89.79	106.67	89.79	106.67
Analytical peak capacity (minimum of flexure and shear capacity), kN	89.79	106.67	89.79	101.68	49.15	50.84
Experimental peak capacity, kN	115.00	124.50	95.50	104.00	43.00	51.00
Experimental failure mode	Diagonal shear tension	Diagonal shear tension	Combined flexure shear	Combined flexure shear	Flexure underreinforced	Flexure underreinforced

Note: HCS = hollow-core slab. 1 kN = 0.225 kip.

V_{wd} = contribution of the shear reinforcement due to stirrups or inclined bars

k = coefficient that allows for the effect of non-uniform self-equilibrating stress

ρ_l = longitudinal reinforcement

f_{fck} = cylinder compressive strength

σ_{cp} = prestressing stress

b_w = minimum width of the section over the effective depth d

A_s = area of tension reinforcement extending not less than d plus the anchorage length beyond the section considered

N_{sd} = prestressing force

A_c = cross-sectional area of concrete

k_f = factor for taking into account the contribution of the flanges in a T section

k_1 = coefficient that takes into account the bond properties of the bars

τ_{fd} = design value of the increase in shear strength due to steel fibers

n = shape factor

b_f = width of the flanges

h_f = height of the flanges

$f_{RK,4}$ = residual flexural tensile strength

A_{sw} = area of shear reinforcement

s = spacing between the shear reinforcement measured along the longitudinal axis

f_{ywd} = design yield strength of the shear reinforcement

α = angle of shear reinforcement with longitudinal axis

The theoretical flexural capacity of the slabs with fibers was calculated by modifying the same equations to account for the load contribution of the fibers in the cross section as a function of the volume fraction of the fibers based on previous studies.[4,11] The ductility of fiber-reinforced concrete in compression is higher due to passive confinement from the structural fibers; thus the use of fibers in concrete creates a distributed confinement system leading to an increase in

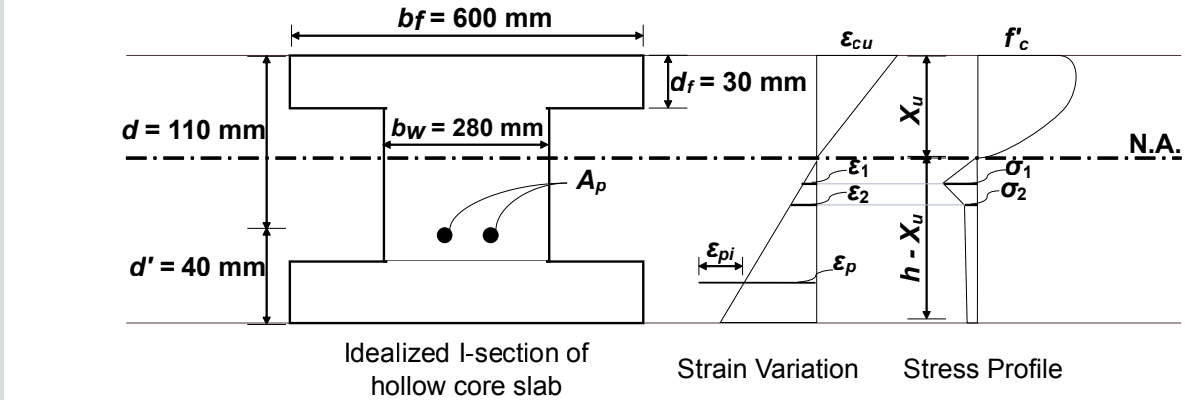

Figure 9. Layer discretization for sectional analysis. Note: 1 in. = 25.4 mm.

ductility at both the material and structural levels.[33] The shear capacity predictions were made using the equation given in *Eurocode 2: Design of Concrete Structures –Part 1-1: General Rules and Rules for Buildings* (EN 1992-1-1)[39] with the proposed design recommendations from *Istruzioni per la Progettazione, l'Esecuzione ed il Controllo di Strutture di Calcestruzzo Fibrorinforzato* (CNR-DT 204/2006).[40] Further details on the equations used for flexure and shear capacity can be found elsewhere.[4,11,35,36] The minimum load required to reach the flexural or shear capacity is taken as the theoretical peak load. Table 5 compares the experimental and analytical calculations. The results show that the analytical models predicted the capacity of slabs with reasonable accuracy.

Scope for further work

The specimens in this study largely exhibited an underreinforced failure through the yielding of strands, followed by concrete compression failure. The behavior of hollow-core slabs with high reinforcement and prestressing ratios would be interesting to study because they may lead to different failure modes. Parameters that were not included in the scope of this study, such as prestressing ratio, concrete strength, and fiber dosages, should also be further studied to develop generic design guidelines. A comparative study on the efficacy of steel and structural synthetic fibers on the shear-dominated behavior of hollow-core slabs is also worth investigating and is scope for further work.

Conclusion

Prestressed hollow-core slabs with and without structural macrosynthetic fiber reinforcement were tested to assess improvements in their performance. Six slabs were tested with varying shear span–to–depth ratio *a*/*d* values. The behavior of the fiber-reinforced hollow-core slabs shows that the addition of fibers is very effective in controlling crack openings and in increasing ductility and energy dissipation. The following conclusions can be drawn from the test results presented in this paper:

- The workability of the zero-slump concrete did not change significantly due to the addition of structural polyolefin fibers.
- Fracture tests revealed that the residual load-bearing capacity of structural polyolefin fibers was best for crack openings in the range of 1 to 5 mm (0.04 to 2 in.). Test results also showed significant improvements in toughness and ductility with the addition of fibers.
- Full-scale structural tests on hollow-core slabs revealed that the addition of fibers increased the peak load carrying capacity. A maximum increase of 19% in peak load was observed in hollow-core slabs tested at an *a*/*d* of 7.5, while slabs with other *a*/*d* values (2.5 and 3.75) had an increase of approximately 9%.
- Synthetic fibers resisted crack openings and reduced the strain in the prestressing strands. At a flexure-dominant *a*/*d* of 7.5, the strain in the strands reduced by 42%, and at an *a*/*d* of 3.75 the strain reduced by 32% for similar load levels after cracking due to the contribution of fibers to load resistance.
- Synthetic fibers increased crack distribution and reduced crack widths at all values of *a*/*d*. A maximum increase of 24% in energy dissipation was observed due to fiber addition because of improved post-peak behavior.
- The effect of fibers is more prominent in flexure-dominating high *a*/*d* specimens than in low *a*/*d* specimens.
- The addition of fibers increased the postcracking stiffness of the slabs by about 40% in slabs with *a*/*d* values of 2.5 and 3.75, indicating better crack bridging by the fibers and leading to better serviceability performance.

Acknowledgments

This study was conducted as part of a project funded by the Uchhatar Avishkar Yojana (UAY) scheme of the Indian government. Their financial support is gratefully acknowledged. We also acknowledge PRECA Ltd. of Hyderabad, India, for their financial support and help in the casting of the hollow-core slabs used in this study. The supply of synthetic fibers provided by GRENIX, India, is also duly acknowledged.

References

1. Cuenca, E., J. Echegaray-Oviedo, and P. Serna. 2015. "Influence of Concrete Matrix and Type of Fiber on the Shear Behavior of Self-Compacting Fiber Reinforced Concrete Beams." *Composites Part B: Engineering* 75: 135–147.

2. Cuenca, E., and P. Serna. 2013. "Shear Behavior of Prestressed Precast Beams Made of Self-Compacting Fiber Reinforced Concrete." *Construction and Building Materials* 45: 145–156.

3. Martinola, G., A. Meda, G. A. Plizzari, and Z. Rinaldi. 2010. "Strengthening and Repair of RC Beams with Fiber Reinforced Concrete." *Cement and Concrete Composites* 32 (9): 731–739.

4. Padmarajaiah, S. K., and A. Ramaswamy. 2004. "Flexural Strength Predictions of Steel Fiber Reinforced High-Strength Concrete in Fully/Partially Prestressed Beam Specimens." *Cement and Concrete Composites* 26 (4): 275–290.

5. Narayanan, R., and I. Y. S. Darwish. 1987. "Shear in Prestressed Concrete Beams Containing Steel Fibers." *International Journal of Cement Composites and Lightweight Concrete* 9 (2): 81–90.

6. Becker, R. J., and D. R. Buettner. 1985. "Shear Tests of Extruded Hollow-Core Slabs." *PCI Journal* 30 (2): 40–54.

7. Pisanty, A. 1992. "The Shear Strength of Extruded Hollow-Core Slabs." *Materials and Structures* 25 (4): 224–230.

8. Hawkins, N. M., and S. K. Ghosh. 2006. "Shear Strength of Hollow-Core Slabs." *PCI Journal* 51 (1): 110–114.

9. Palmer, K. D., and A. E. Schultz. 2011. "Experimental Investigation of the Web-Shear Strength of Deep Hollow-Core Units." *PCI Journal* 56 (4): 83–104.

10. Paine, K. A. 1998. "Steel Fibre Reinforced Concrete for Prestressed Hollow Core Slabs." PhD diss., University of Nottingham, UK.

11. Paine, K. A., K. S. Elliott, and C. H. Peaston. 1997. "Increasing the Shear Strength and Ductility of Hollow Core Slabs Using Metal Fibers." In *International Symposium on Noteworthy Developments in Prestressing and Precasting*. Edited by T. W. Leong and J. S. Y. Tan. Singapore: CI-Premier.

12. Peaston, C., K. Elliot, and K. Paine. 1999. "Steel Fiber Reinforcement for Extruded Prestressed Hollow Core Slabs." *ACI Special Publication* 182: 87–108.

13. Simasathien, S., and S.-H. Chao. 2015. "Shear Strength of Steel-Fiber-Reinforced Deep Hollow-Core Slabs." *PCI Journal* 60 (4): 85–101.

14. Cuenca, E., and P. Serna. 2013. "Failure Modes and Shear Design of Prestressed Hollow Core Slabs Made of Fiber-Reinforced Concrete." *Composites Part B: Engineering* 45 (1): 952–964.

15. Marazzini, M., and G. Rosati. 1999. "Fiber Reinforced High-Performance Concrete Beams Material and Structural Behavior." *ACI Special Publication* 182: 29–52.

16. Jain, S., S. S. Prakash, and K. V. L. Subramaniam. 2016. "Monitoring of Concrete Cylinders with and Without Steel Fibers under Compression Using Piezo-Ceramic Smart Aggregates." *Journal of Nondestructive Evaluation* 35 (59). https://doi.org/10.1007/s10921-016-0376-2.

17. Srikar, G., G. Anand, and S. S. Prakash. 2016. "A Study on Residual Compression Behavior of Structural Fiber Reinforced Concrete Exposed to Moderate Temperature Using Digital Image Correlation." *International Journal of Concrete Structures and Materials* 10 (1): 75–85.

18. Pachalla, S. K. S., and S. S. Prakash. 2017. "Experimental Evaluation on Effect of Openings on Behavior of Prestressed Precast Hollow-Core Slabs." *ACI Structural Journal* 114 (2): 427–436.

19. Pachalla, S. K. S., and S. S. Prakash. 2017. "Load Resistance and Failure Modes of GFRP Composite Strengthened Hollow Core Slabs with Openings." *Materials and Structures* 50 (3). https://doi.org/10.1617/s11527-016-0883-8.

20. Kankeri, P., and S. S. Prakash. 2016. "Experimental Evaluation of Bonded Overlay and NSM GFRP Bar Strengthening on Flexural Behavior of Precast Prestressed Hollow Core Slabs." *Engineering Structures* 120: 49–57.

21. Kankeri, P., and S. S. Prakash. 2017. "Efficient Hybrid Strengthening for Precast Hollow Core Slabs at Low and High Shear Span to Depth Ratios." *Composite Structures* 170: 202–214.

22. Joshi, S., N. Thammishetti, and S. S. Prakash. 2018. "Ef-

ficiency of Steel and Macro-Synthetic Structural Fibers on the Flexure-Shear Behavior of Prestressed Concrete Beams." *Engineering Structures* 171: 47–55.

23. Olivito, R. S., and F. A. Zuccarello. 2010. "An Experimental Study on the Tensile Strength of Steel Fiber Reinforced Concrete." *Composites Part B: Engineering* 41 (3): 246–255.

24. Soulioti, D. V., N. M. Barkoula, A. Paipetis, and T. E. Matikas. 2011. "Effects of Fibre Geometry and Volume Fraction on the Flexural Behavior of Steel-Fibre Reinforced Concrete." *Strain* 47 (s1): e535–e541.

25. Barros, J. A. O., and J. A. Fueiras. 1999. "Flexural Behavior of SFRC: Testing and Modeling." *Journal of Materials in Civil Engineering* 11 (4): 331–339.

26. Li, V. C. 2002. "Large Volume, High-Performance Applications of Fibers in Civil Engineering." *Journal of Applied Polymer Science* 83 (3): 660–686.

27. Rasheed, M. A., Y. Kawasaki, S. S. Prakash, and N. Ogawa. 2017. "Acoustic Emission Behavior of Synthetic Fiber Reinforced Concrete under Flexure." In *International Conference on Advances in Construction Materials and Systems: Proceedings,2017, Chennai, India*. Paris, France: RILEM (International Union of Laboratories and Experts in Construction Materials, Systems and Structures).

28. Cifuentes, H., F. García, O. Maeso, and F. Medina. 2013. "Influence of the Properties of Polypropylene Fibers on the Fracture Behavior of Low-, Normal-and High-Strength FRC." *Construction and Building Materials* 45: 130–137.

29. Lanzoni, L., A. Nobili, and A. M. Tarantino. 2012. "Performance Evaluation of a Polypropylene-Based Draw-Wired Fibre for Concrete Structures." *Construction and Building Materials* 28 (1): 798–806.

30. Buettner, D. R., and R. J. Becker. 1998. *PCI Manual for the Design of Hollow Core Slabs*. MNL-126. 2nd ed. Chicago, IL: PCI.

31. Kani, G. N. J. 1967. "How Safe Are Our Large Reinforced Concrete Beams?" *ACI Structural Journal* 64 (3): 128–141.

32. Devalapura, R. K., and M. K. Tadros. 1992. "Stress-Strain Modeling of 270 ksi Low-Relaxation Prestressing Strands." *PCI Journal* 37 (2): 100–106.

33. Fantilli, A. P., and B. Chiaia. 2017. "Conventional and Unconventional Approaches for the Evaluation of Crack Width in FRC Structures." *ACI Special Publication* 319: 4.1–4.12.

34. Haus, A. 2017. "From Theory to Practice–15 Years of Applying SFRC for Crack Control in Design." *ACI Special Publication* 319: 8.1–8.12.

35. Carreira, D. J., and K.-H. Chu. 1985. "Stress-Strain Relationship for Plain Concrete in Compression." *Journal of the American Concrete Institute* 82 (6): 797–804.

36. Ou, Y.-C., M.-S. Tsai, K.-Y. Liu, and K.-C. Chang. 2011. "Compressive Behavior of Steel-Fiber-Reinforced Concrete with a High Reinforcing Index." *Journal of Materials in Civil Engineering* 24 (2): 207–215.

37. Amin, A., S. J. Foster, R. I. Gilbert, and W. Kaufmann. 2017. "Material Characterization of Macro Synthetic Fibre Reinforced Concrete." *Cement and Concrete Composites* 84: 124–133.

38. RILEM Technical Committee 162-TDF. 2002. "Bending Test: Final Recommendation." *Materials and Structures* 35 (9): 579–582.

39. CEN (European Committee for Standardization) Technical Committee CEN/TC250. 2004. *Eurocode 2: Design of Concrete Structures – Part 1-1: General Rules and rules for Buildings*. EN-1992-1-1. Brussels, Belgium: CEN.

40. CNR (Consiglio Nazionale Delle Ricerche). 2006. *Istruzioni per la Progettazione, l'Esecuzione ed il Controllo di Strutture di Calcestruzzo Fibrorinforzato*. CNR-DT 204/2006. Rome, Italy: CNR.

Notation

a = shear span

A_c = cross-section area of concrete

A_s = area of tension reinforcement extending not less than d plus the anchorage length beyond the section considered

A_{sw} = area of shear reinforcement

b_f = width of the flanges

b_w = minimum width of the section over the effective depth d

d = effective depth

f_{fck} = cylinder compressive strength

$f_{Rk,4}$ = residual flexural tensile strengths at crack mouth opening displacement

f_{ywd} = design yield strength of the shear reinforcement

h_f = height of the flanges

k = coefficient that allows for the effect of nonuniform self-equilibrating stress

k_1 = coefficient that takes into account the bond properties of the bars

k_f = factor for taking into account the contribution of the flanges in a T section

n = shape factor

N_{sd} = longitudinal force in section due to loading or prestressing

s = spacing between the shear reinforcement measured along the longitudinal axis

V_{cd} = shear resistance of the member without shear reinforcement

V_{fd} = contribution of the steel fiber shear reinforcement

V_{Rd3} = design shear resistance of a section of a beam

V_{wd} = contribution of the shear reinforcement due to stirrups or inclined bars

α = angle of the shear reinforcement with the longitudinal axis

τ_{fd} = design value of the increase in shear strength due to steel fibers

ρ_l = longitudinal reinforcement

σ_{cp} = prestressing stress

About the authors

Pradeep Kankeri, PhD, is an associate professor in the Department of Civil Engineering at Vardhaman College of Engineering in Hyderabad, India. He received his PhD from the Indian Institute of Technology Hyderabad (IIT Hyderabad) in Telangana, India. His research interests include the behavior of reinforced and prestressed concrete and the use of fiber-reinforced polymer (FRP) composites in construction.

Sameer K. S. Pachalla, PhD, is a postdoctoral research associate in the Department of Civil, Construction and Environmental Engineering at Iowa State University in Ames, Iowa. He received his PhD from IIT Hyderabad. His research interests include the development of precast concrete wind towers, the behavior of reinforced and prestressed concrete members, and strengthening of concrete members using FRP composites.

Nikesh Thammishetti is a research scholar in the Structural Engineering Division of IIT Hyderabad. He received his bachelor of technology degree from Kakatiya Institute of Technology and Science in Warangal, India, and his master's degree from Birla Institute of Technology in Pilani, India. His research interests include the mechanics of reinforced concrete and the repair and rehabilitation of reinforced concrete structures using innovative ductile materials.

S. Suriya Prakash, PhD, is an associate professor in the Department of Civil Engineering at IIT Hyderabad. He is a recipient of the prestigious Ramanujan Fellowship from the Government of India. Before joining IIT Hyderabad, he worked as a design engineer at Structural Group Inc. in Baltimore, Md. He received his PhD from the Missouri University of Science and Technology in Rolla, Mo. His research interests include precast/prestressed concrete and seismic design and retrofit of reinforced concrete and masonry structures using advanced construction materials.

Abstract

Prestressed hollow-core slabs are generally precast concrete elements manufactured using an extrusion machine. Although prestressed hollow-core slabs are designed as uncracked members under service loads, cracking is unavoidable under excessive loading. The postcracking behavior of hollow-core slabs can be improved at very low cost by adding structural macrosynthetic fibers during the casting process with no modifications to the mixture proportions of zero-slump concrete. This paper examines the behavior of structural macrosynthetic fiber-reinforced hollow-core slabs at three different shear span–to–depth ratios *a*/*d*. Six full-scale tests were conducted on hollow-core slabs, of which three had no fiber additives and three had a polyolefin fiber dosage of 0.33%. The *a*/*d* values of 2.5, 3.75, and 7.5 were considered to evaluate the effect of macrofibers on the performance of hollow-core slabs. The test results indicate that the addition of macrosynthetic fibers increased the ultimate strength up to 19% with an increase in ductility. The contribution of fibers in improving the postcracking stiffness was better at higher *a*/*d* values under flexure-dominant behavior. Existing analytical models were suitably modified to predict the theoretical capacity of slabs with and without fibers.

Keywords

Fiber reinforced, hollow-core slab, macrosynthetic fiber, prestressed, shear span–to–depth ratio.

Review policy

This paper was reviewed in accordance with the Precast/Prestressed Concrete Institute's peer-review process.

Reader comments

Please address any reader comments to *PCI Journal* editor-in-chief Emily Lorenz at elorenz@pci.org or Precast/Prestressed Concrete Institute, c/o *PCI Journal*, 200 W. Adams St., Suite 2100, Chicago, IL 60606.